Since January 2020 Elsevier has created a COVID-19 resource centre with free information in English and Mandarin on the novel coronavirus COVID-19. The COVID-19 resource centre is hosted on Elsevier Connect, the company's public news and information website.

Clinical Imaging 80 (2021) 229–238

Contents lists available at ScienceDirect

Clinical Imaging

journal homepage: www.elsevier.com/locate/clinimag

Cardiothoracic Imaging

Systematic review and meta-analysis of chest radiograph (CXR) findings in COVID-19

Zuhair Sadiq *, Shehroz Rana, Ziyad Mahfoud, Ameed Raoof

Weill Cornell Medicine-Qatar, Education City, Qatar Foundation, Doha, Qatar

ARTICLE INFO

Keywords:
COVID-19
Imaging
Chest radiograph
CXR
Coronavirus
SARS-CoV-2
Meta-analysis

ABSTRACT

Chest radiography (CXR) is most likely to be the utilized modality for diagnosing COVID-19 and following up on any lung-associated abnormalities. This review provides a meta-analysis of the current literature on CXR imaging findings to determine the most common appearances of lung abnormalities in COVID-19 patients in order to equip medical researchers and healthcare professionals in their efforts to combat this pandemic. Twelve studies met the inclusion criteria and were analyzed. The inclusion criteria consisted of: (1) published in English literature; (2) original research study; (3) sample size of at least 5 patients; (4) reporting clinical characteristics of COVID-19 patients as well as CXR imaging features; and (5) noting the number of patients with each corresponding imaging feature. A total of 1948 patients were included in this study. To perform the meta-analysis, a random-effects model calculated the pooled prevalence and 95% confidence intervals of abnormal CXR imaging findings. Seventy-four percent (74%) (95% CI: 51–92%) of patients with COVID-19 had an abnormal CXR at the initial time of diagnosis or sometime during the disease course. While there was no single feature on CXR that was diagnostic of COVID-19 viral pneumonia, a characteristic set of findings were obvious. The most common abnormalities were consolidation (28%, 95% CI: 8–54%) and ground-glass opacities (29%, 95% CI: 10–53%). The distribution was most frequently bilateral (43%, 95% CI: 27–60%), peripheral (51%, 95% CI: 36–66%), and basal zone (56%, 95% CI: 37–74%) predominant. Contrary to parenchymal abnormalities, pneumothorax (1%, 95% CI: 0–3%) and pleural effusions (6%, 95% CI: 1–16%) were rare.

1. Introduction

The first case of coronavirus disease 2019 (COVID-19) was first reported in Wuhan, China in December 2019 and it was declared a pandemic by the World Health Organization (WHO) in March 2020[1]. Healthcare workers need diagnostic tools to study cases of potential COVID-19 that are both sensitive and specific[7]. The gold standard for diagnosing COVID-19 patients is a viral nucleic acid test conducted by reverse transcription-polymerase chain reaction (RT-PCR) with a sensitivity of 79% and specificity of 100%[2]. Chest CT has been found to have comparable diagnostic performance with a sensitivity of 77% and specificity of 96%[3].

The pulmonary system is primarily affected by COVID-19, as such, it is common practice to request a chest radiograph (CXR) in suspicious cases as the initial imaging exam. The diagnostic performance of CXR in the early stages of COVID-19 is, however, limited and pathological findings may not be detected on radiography that is identifiable on chest CT[8]. CXR obtained from confirmed and symptomatic COVID-19 patients have had a lower sensitivity at 69%[4]. Although CXR is less sensitive, it is available in urgent care centers, clinics and hospitals and may help with COVID-19 diagnosis[7].

Available information on CXR features of COVID-19 is dispersed among various published papers in the scientific literature, and a consolidated systematic review has yet to be assembled. This review intends to analyze the characteristics of the rapidly progressive COVID-19 viral pneumonia on CXR. The value of radiographic imaging is in generating results that are clinically actionable either for establishing a diagnosis or for guiding patient management. We aim to determine the most common appearances of lung abnormalities in COVID-19 patients to provide insight into the initial CXR as well as follow-up CXR characteristics of this infectious disease. The characteristic imaging findings during the different stages of the disease and the variation in the

Abbreviations: ES, Effect size; CI, Confidence interval; COVID-19, Coronavirus disease of 2019; CT, Computed tomography; CXR, Chest X-ray; GGO, Ground-glass opacity; ICU, Intensive care unit; RT-PCR, Reverse transcription polymerase chain reaction.

* Corresponding author.
E-mail address: zys4001@qatar-med.cornell.edu (Z. Sadiq).

https://doi.org/10.1016/j.clinimag.2021.06.039
Received 28 December 2020; Received in revised form 24 June 2021; Accepted 30 June 2021
Available online 27 July 2021

prevalence of the different patterns are also studied. A review detailing the most common patterns of lung abnormalities on CXR will help equip medical researchers and healthcare professionals in their efforts to combat this pandemic.

2. Methods

2.1. Literature search

This meta-analysis was conducted using "Preferred Reporting Items for Systematic Reviews and Meta-Analyses guidelines"[9]. It includes a systematic literature search of the World Health Organization database, PubMed, Elsevier and Google Scholar, using the keywords "COVID-19 OR coronavirus OR SARS-Cov-2" and "chest x-ray OR CXR".

2.2. Eligibility criteria

The resulting studies that meet the following inclusion criteria were included in this review's analysis: (1) published in English literature; (2) original research study; (3) sample size of at least 5 patients; (4) reporting clinical characteristics of COVID-19 patients as well as CXR imaging features; and (5) noting the number of patients with each corresponding imaging feature. Studies that lacked research data or outcome parameters were excluded.

2.3. Data extraction

An aggregate of 401 non-duplicate citations was identified by using the aforementioned search strategies from which 37 potentially applicable papers were evaluated. Ultimately, 12 studies were eligible with reported cases ranging from 5 to 636 were included in the meta-analysis (Tables 1, 2 & 3). In total, these studies contained 1948 patients, 643 cases with normal CXR and 1305 cases with abnormal CXR findings (Fig. 1). Table 1 contains the basic demographic of the participant population in each study as well as the reported CXR findings.

In the following sections, we present an analysis and review of CXR findings in COVID-19 patients as gathered from the eligible studies. The ensuing info was collected from each published paper for the analysis of CXR findings: total number of patients in the study; gender of participants and average age; lung lesion distribution (diffuse, peripheral or perihilar); lung involvement (right, left, or bilateral); typical abnormalities such as consolidation and ground-glass opacities; frequency of zone predominance (superior or basal); and less common findings such as pleural effusion, pulmonary edema, atelectasis and pneumothorax. Stata version 15.0 was utilized to perform the statistical analysis. Tables 1 and 2 summarize the collected data. The figures displaying the CXR findings were obtained with permission via email from *Radiopedia.org*.

2.4. Statistical analysis

A meta-analysis was conducted using a variance components model to determine the pooled proportion values and the analogous 95% confidence intervals (CI) of distinctive imaging features linked to patients with COVID-19. The pooled-effects meta-analysis model involved an assumption that the effect size (ES) being approximated in the different studies are not alike; rather, they adhere to some distribution (Fig. 1). The center of the symmetric distribution characterizes the average of the effects, whilst the width describes the degree of heterogeneity[10]. Statistical heterogeneity was calculated using the I^2 test ($p < 0.05$ represented significant statistical heterogeneity). Data was entered into Stata version 15.0 to perform statistical analyses.

The pooled-effects model was calculated for each CXR finding. All the graphs for the meta-analyses and forest plots can be found in the supplementary document. Statistically significant heterogeneity was found among all the studies in regards to the data extracted from their findings ($p < 0.05$). The results from the graphs were summarized in Table 3.

3. Results

CXR was utilized in 12 studies diagnosing COVID-19. Both CXR and CT were used in 4 studies, with chest CT proving to be superior to CXR in the assessment and detection of each type of lung abnormality,

Table 1
Basic clinical characteristics of studies in COVID-19 patients.

Reference	Country of Origin	Date Published (d/m/y)	Number of Participants	Gender Male: Female	Average Age	Method of Diagnosis	Patient Type	Symptom Severity	Onset of symptoms prior to radiograph taken
Arentz et al.	USA	28/4/2020	21	11:10	70	RT-PCR	Inpatient	SOB (76%), fever (52%), cough (48%)	3.5 days
Chen et al.	China	30/1/2020	99	67:32	55.5	RT-PCR (by WHO interim guidance)	Inpatient	Cough and fever (82%), SOB (30%)	–
Cozzi et al.	Italy	9/6/2020	234	153:81	66	RT-PCR	Inpatient	–	–
Guan et al.	China	30/4/2020	274	–	47.0	RT-PCR	Inpatient	Fever (88.7%), cough (67.8%)	4 days
Ippolito et al.	Italy	22/4/2020	468	328:140	64.7	RT-PCR	Inpatient	Fever (90.6%), cough (57.7%), dyspnea (56.8%)	>5 days for majority of patients (57.7%)
Kim et al.	Korea	6/4/2020	28	–	42.6	RT-PCR	Inpatient	Cough (28.6%), sore throat (28.6), fever, myalgia, and headache (25%)	–
Ng et al.	China	2/2/2020	5	–	56	RT-PCR	–	Fever (90%), cough (48%), sore throat (10%), diarrhea (10%)	3
Russel et al.	USA	–/5/2020	636	363:273	50	RT-PCR	–	–	–
Toussie et al.	USA	14/5/2020	338	210:128	39	RT-PCR	Inpatient	–	4 days
Vancheri et al.	Italy	30/5/2020	240	169:71	65	RT-PCR	Inpatient	–	–
Wong et al.	China	27/5/2020	64	26:38	56	RT-PCR	Inpatient	Fever (59%), cough (41%), asymptomatic (14%)	10–12 days
Yoon et al.	Korea	21/4/2020	9	4:5	54	RT-PCR	Inpatient	–	–

Table 2
Chest radiograph findings of studies in COVID-19 patients.

Reference	Baseline			Lung Involvement			Consolidation *(%)*	Ground Glass Opacities *(%)*	Distribution			Zone Predominance			Other Atypical Features *(%)*
	Normal *(%)*	Abnormal *(%)*	Normal Turned Abnormal *(%)*	Right *(%)*	Left *(%)*	Bilateral *(%)*			Diffuse *(%)*	Peripheral *(%)*	Perihilar *(%)*	None *(%)*	Superior *(%)*	Basal *(%)*	
Arentz et al.	1 *(4.8)*	20 *(95.2)*	0 *(0)*	–	–	11 *(52.4)*	4 *(19.0)*	10 *(47.6)*	–	–	–	–	–	–	Pleural Effusion: 6 *(28.6)* Pulmonary Edema: 2 *(9.5)* Atelectasis: 1 *(4.8)*
Chen et al.	0 *(0)*	99 *(100)*	0 *(0)*	–	–	74 *(74.7)*	–	14 *(14.1)*	–	–	–	–	–	–	Pneumothorax: 1 *(1)*
Cozzi et al.	13 *(5.6)*	221 *(94.4)*	0 *(0)*	29 *(12.4)*	21 *(9.0)*	162 *(69.2)*	135 *(57.7)*	147 *(62.8)*	37 *(16.5)*	135 *(60.5)*	51 *(22.8)*	55 *(24.6)*	31 *(13.9)*	137 *(61.4)*	Cardiomegaly: 70 *(29.9)* Pleural Effusion: 39 *(16.7)* Pneumothorax: 5 *(2.4)*
Guan et al.	112 *(40.9)*	162 *(59.1)*	0 *(0)*	–	–	100 *(36.5)*	–	55 *(20.1)*	–	–	–	–	–	–	–
Ippolito et al.	–	–	–	–	–	301 *(64.5)*	245 *(52.5)*	335 *(63.1)*	–	292 *(62.5)*	–	–	–	335 *(71.1)*	Pleural Effusion: 57 *(12.2)*
Kim et al.	15 *(53.6)*	13 *(46.4)*	0 *(0)*	–	–	6 *(21.4)*	–	–	–	–	–	–	–	–	–
Ng et al.	2 *(40.0)*	3 *(60.0)*	0 *(0)*	–	–	2 *(40.0)*	3 *(60.0)*	–	–	–	–	2 *(40.0)*	0 *(0)*	1 *(20.0)*	–
Russel et al.	371 *(58.3)*	265 *(41.7)*	0 *(0)*	–	–	133 *(20.9)*	34 *(5.3)*	120 *(18.9)*	6 *(0.9)*	225 *(35.4)*	45 *(7.1)*	6 *(0.9)*	128 *(20.1)*	215 *(33.8)*	Pleural Effusion: 2 *(0.3)*
Toussie et al.	–	–	–	–	–	–	–	–	–	–	–	–	23 *(6.8)*	270 *(79.9)*	Pleural Effusion: 0 *(0)* Pneumothorax: 0 *(0)*
Vancheri et al.	60 *(25.0)*	180 *(75.0)*	0 *(0)*	24 *(10.0)*	24 *(10.0)*	132 *(55.0)*	71 *(29.6)*	124 *(51.7)*	71 *(29.6)*	89 *(37.1)*	20 *(8.3)*	–	66 *(27.5)*	158 *(65.8)*	Pleural Effusion: 12 *(5.0)*
Wong et al.	20 *(31.3)*	44 *(68.8)*	7 *(10.9)*	10 *(15.6)*	9 *(14.1)*	32 *(50.0)*	30 *(46.8)*	21 *(32.8)*	19 *(29.7)*	26 *(40.6)*	6 *(9.4)*	19 *(29.7)*	0 *(0)*	32 *(50.0)*	Pleural Effusion: 2 *(3)*
Yoon et al.	4 *(44.4)*	5 *(55.6)*	0 *(0)*	5 *(55.6)*	5 *(55.6)*	–	8 *(88.9)*	2 *(22.2)*	2 *(22.2)*	6 *(66.6)*	2 *(22.2)*	–	2 *(22.2)*	5 *(55.6)*	–

Table 3
Compilation of pooled prevalence of chest radiograph imaging findings from each study.

Meta-Analyses: Pooled Prevalence of CXR Imaging Findings (95% CI)															
Reference	Baseline			Lung Involvement			Consolidation	Ground Glass Opacities	Distribution			Zone Predominance			Pleural Effusion
	Normal	Abnormal	Normal Turned Abnormal	Right	Left	Bilateral			Diffuse	Peripheral	Perihilar	None	Superior	Basal	
Arentz et al.	0.05 *(0.00, 0.24)*	0.95 *(0.76, 1.00)*	0.00 *(0.00, 0.16)*	–	–	0.52 *(0.30, 0.74)*	0.19 *(0.05, 0.42)*	0.48 *(0.26, 0.70)*	–	–	–	–	–	–	0.29 *(0.11, 0.52)*
Chen et al.	0.00 *(0.00, 0.04)*	1.00 *(0.96, 1.00)*	0.00 *(0.00, 0.04)*	–	–	0.75 *(0.65, 0.83)*	–	0.14 *(0.08, 0.23)*	–	–	–	–	–	–	–
Cozzi et al.	0.06 *(0.00, 0.09)*	0.94 *(0.91, 0.97)*	0.00 *(0.00, 0.02)*	0.12 *(0.08, 0.17)*	0.09 *(0.06, 0.13)*	0.69 *(0.63, 0.75)*	0.58 *(0.51, 0.64)*	0.63 *(0.56, 0.69)*	0.16 *(0.11, 0.21)*	0.58 *(0.51, 0.64)*	0.22 *(0.17, 0.28)*	0.24 *(0.18, 0.29)*	0.13 *(0.09, 0.18)*	0.59 *(0.52, 0.65)*	0.17 *(0.12, 0.22)*
Guan et al.	0.41 *(0.35, 0.47)*	0.59 *(0.53, 0.65)*	0.00 *(0.00, 0.01)*	–	–	0.36 *(0.31, 0.43)*	–	0.20 *(0.15, 0.25)*	–	–	–	–	–	–	–
Ippolito et al.	–	–	–	–	–	0.64 *(0.60, 0.69)*	0.52 *(0.48, 0.57)*	0.72 *(0.67, 0.76)*	–	0.62 *(0.59, 0.67)*	–	–	–	0.72 *(0.67, 0.76)*	0.12 *(0.09, 0.15)*
Kim et al.	0.54 *(0.34, 0.72)*	0.46 *(0.28, 0.66)*	0.00 *(0.00, 0.12)*	–	–	0.21 *(0.08, 0.41)*	–	–	–	–	–	–	–	–	–
Ng et al.	0.40 *(0.05, 0.85)*	0.60 *(0.15, 0.95)*	0.00 *(0.00, 0.52)*	–	–	0.40 *(0.05, 0.85)*	0.60 *(0.15, 0.95)*	–	–	–	–	0.40 *(0.05, 0.85)*	0.00 *(0.00, 0.52)*	0.20 *(0.01, 0.72)*	–
Russel et al.	0.58 *(0.62, 0.54)*	0.42 *(0.38, 0.46)*	0.00 *(0.00, 0.01)*	–	–	0.21 *(0.18, 0.24)*	0.05 *(0.04, 0.07)*	0.19 *(0.16. 0.22)*	0.01 *(0.00, 0.02)*	0.35 *(0.32, 0.39)*	0.07 *(0.05, 0.09)*	0.01 *(0.00, 0.02)*	0.20 *(0.17, 0.23)*	0.34 *(0.30, 0.38)*	0.00 *(0.00. 0.01)*
Toussie et al.	–	–	–	–	–	–	–	–	–	–	–	–	0.07 *(0.04, 0.10)*	0.80 *(0.75, 0.84)*	0.00 *(0.00. 0.01)*
Vancheri et al.	0.25 *(0.20, 0.31)*	0.75 *(0.69, 0.80)*	0.00 *(0.00, 0.02)*	0.10 *(0.07, 0.15)*	0.10 *(0.07, 0.15)*	0.55 *(0.49, 0.61)*	0.30 *(0.24, 0.36)*	0.52 *(0.45, 0.58)*	0.30 *(0.24, 0.36)*	0.37 *(0.31, 0.44)*	0.08 *(0.05, 0.13)*	–	0.28 *(0.22, 0.34)*	0.66 *(0.59, 0.72)*	0.05 *(0.02, 0.09*
Wong et al.	0.31 *(0.20, 0.44)*	0.69 *(0.56, 0.80)*	0.11 *(0.05, 0.21)*	0.16 *(0.08, 0.27)*	0.14 *(0.07, 0.25)*	0.50 *(0.37, 0.63)*	0.47 *(0.34, 0.60)*	0.33 *(0.22, 0.46)*	0.30 *(0.19, 0.42)*	0.41 *(0.29, 0.54)*	0.09 *(0.04, 0.19)*	30 *(0.19, 0.42)*	0.00 *(0.00, 0.06)*	0.50 *(0.37, 0.63)*	0.03 *(0.00, 0.11)*
Yoon et al.	0.44 *(0.14, 0.79)*	0.56 *(0.21, 0.86)*	0.00 *(0.00, 0.34)*	0.56 *(0.21, 0.86)*	0.56 *(0.21, 0.86)*	–	0.89 *(0.52, 1.00)*	0.22 *(0.03, 0.60)*	0.22 *(0.03, 0.60)*	0.67 *(0.30, 0.93)*	0.22 *(0.03, 0.60)*	–	0.22 *(0.03, 0.60)*	0.56 *(0.21, 0.86)*	–
Overall I^2	98.18%	98.18%	70.54%	76.22%	91.48%	97.54%	99.03%	99.14%	97.19%	95.67%	91.07%	98.01%	92.14%	97.79%	97.41%
Overall *p*	0.00	0.00	0.00	0.01	0.00	0.00	0.00	0.00	0.00	0.00	0.00	0.00	0.00	0.00	0.00

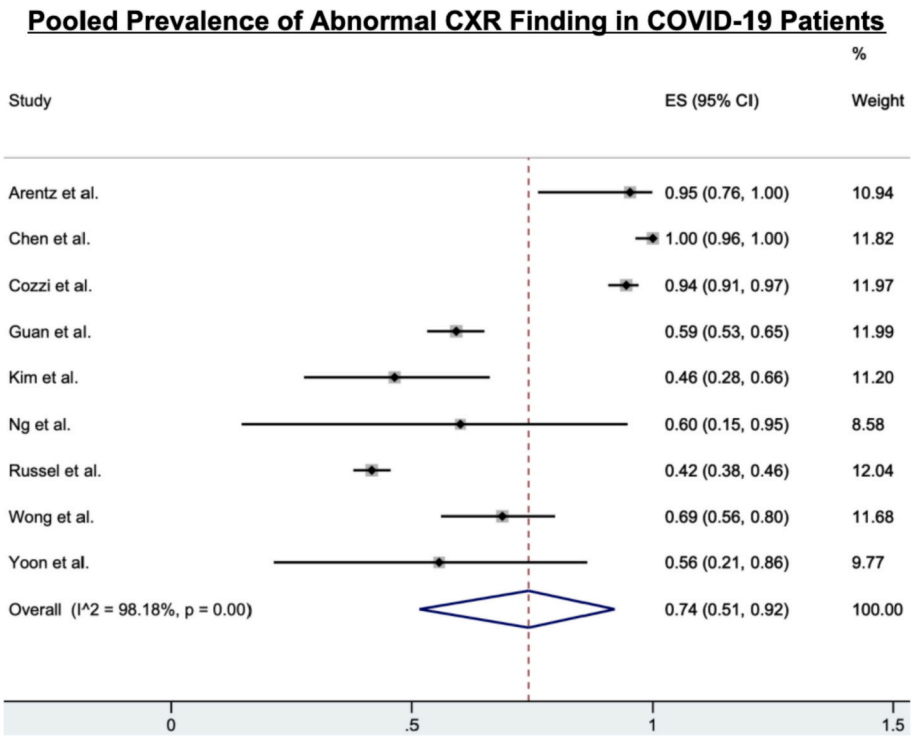

Fig. 1. A forest plot illustrating results of the meta-analysis on pooled prevalence values for abnormal CXR in COVID-19 patients. Each study is represented by one line in this figure, depicting the 95% CIs, and each box in the center describes the proportion for that study comparison. The effect size of each box to the hollow blue diamond represents the strength or the weight that particular study gives to the overall meta-analysis (% Weight). The hollow blue diamond denotes the prevalence value from the pooled-effects model; the center of the diamond gives the overall proportion while the extremities illustrate the 95% CI. (For interpretation of the references to color in this figure legend, the reader is referred to the web version of this article.)

demonstrating the limitations of CXR[11–14]. There is some heterogeneity between studies in regards to the average age of the patient cohort. In addition, the diverse array of findings on CXR sometimes made it hard to make sense of because of vague and nonstandard terminology such as "patchy opacities," "nodules," "infiltrates," "airspace disease," and "airspace opacities", which may contribute to the limitations in CXR analysis.

Of the 12 studies, 9 (75.0%) found normal CXR findings in COVID-19 patients. The proportion of patients with normal CXR findings varied from 5% at the low end of the spectrum to 58% at the higher end; this range was found to be dependent on how COVID-19 presented in patients, with high normal CXR percentages being reported in asymptomatic patients or those with mild symptoms. The overall pooled prevalence was 26% (95% CI: 8–49%). Furthermore, ≥25% of normal CXR findings was reported in 70.0% (7/10) studies. A total of 11 studies (91.7%) noted information in regards to bilateral, right, or left lung involvement (Table 1); from which 9 studies noted a greater proportion of bilateral lung involvement (43%, 95% CI: 27–60%) when compared to right lung involvement (19%, 95% CI: 7–33%) or left lung involvement (1%, 95% CI: 0–4%) (Tables 3 and 4). All 11 studies noted that bilateral lung involvement was more commonly seen in urgent or severe cases of COVID-19 and that bilateral lung involvement was much greater than the involvement of the right or left lung in COVID-19 patients.

Six studies (50.0%) noted the proportions on the distribution of lesions or abnormalities in the perihilar or peripheral lung regions or diffuse lung distribution on CXR, with peripheral distribution (51%, 95% CI: 36–66%) showing significant dominance compared to perihilar distribution (13%, 95% CI: 4–24%) and diffuse distribution (13%, 95% CI: 1–35%). Eight studies (66.7%) reported the details of zone predominance of abnormalities or lesions in the basal or superior or neither lung regions, with basal predominance (56%, 95% CI: 37–74%) being a more common finding compared to superior predominance (8%, 95% CI: 2–16%) or no predominance (17%, 95% CI: 0–46%). Ippolito et al. noted information only on the involvement of peripheral lung distribution and basal predominance[15].

Consolidation and ground-glass opacities (GGOs) were reported in 83.3% (10/12) of the studies; they were the most frequent, atypical abnormalities (Table 1). The pooled prevalence of both consolidation (28%, 95% CI: 8–54%) and GGO (29%, 95% CI: 10–53%) were similar (Table 4). The other two studies did not report any data on these features[16,17]. Besides for consolidation and GGOs, other lung abnormalities were reported in 75.0% (8/12) of these studies, including less common findings like pleural effusion (6%, 95% CI: 1–16%; Fig. 5a) and pneumothorax (1%, 95% CI: 0–3%; Fig. 5b).

3.1. COVID-19 imaging features

3.1.1. Consolidation

One of the most common abnormalities seen on CXR in COVID-19 patients is consolidation. Consolidation refers to an occupation of the air space that causes filling of the alveolar spaces by pathological products such as water, pus and blood in the lungs. It appears as a homogeneous increase in pulmonary parenchymal attenuation (increased density) that obscures the margins of the vessels and the walls of the airways[18]. It may present with an air bronchogram, referring to the visualization of the air bronchial lumens within a parenchymal opacity of the lung and, therefore, implies airway patency[18]. On CXR, it appears to have indistinct margins and presents as fluffy opacities that become confluent over time, so the air that normally surrounds the bronchi becomes opacified and appears white, while the bronchi remain air filled and appear like black tubular structures within the area of consolidation. In Fig. 2a, linear black tubular structures that represent air bronchograms are visible in the left lower lobe and this is one of the key features of consolidation.

3.1.2. Ground glass opacities

Ground-glass opacities (GGOs) describe the lung parenchymal opacification that produces a minor increase in attenuation for the consolidation (Fig. 3). As such, despite the increase in density, the walls of the bronchi and the pulmonary vessels remain differentiated from the affected parenchyma[18]. GGOs represent a partial occupation of the airspace; they are less opaque than consolidations and, as an important consequence, the CT is more sensitive in its detection than CXR. GGOs are common in earlier presentations and can potentially precede the

Table 4
Overall summary of meta-analyses of chest radiograph imaging findings.

Summary: Pooled Prevalence of CXR Imaging Findings														
Overall	Baseline			Lung Involvement			Consolidation	Ground Glass Opacities	Distribution			Zone Predominance			Pleural Effusion
	Normal	Abnormal	Normal Turned Abnormal	Right	Left	Bilateral			Diffuse	Peripheral	Perihilar	None	Superior	Basal	
ES	0.26	0.74	0.00	0.19	0.01	0.43	0.28	0.29	0.13	0.51	0.13	0.17	0.08	0.56	0.06
95% CI	(0.08, 0.49)	(0.51, 0.92)	(0.00, 0.01)	(0.07, 0.33)	(0.00, 0.04)	(0.27, 0.60)	(0.08, 0.54)	(0.10, 0.53)	(0.01, 0.35)	(0.36, 0.66)	(0.04, 0.24)	(0.00, 0.46)	(0.02, 0.16)	(0.37. 0.74)	(0.01, 0.16)

(a) Consolidation (arrows) in the left lower lung zone [25]

(b) Vertical air space consolidation along the left costal margin [27]

(c) Dense consolidation in the right lower zone [25]

Fig. 2. Cases illustrative of consolidation on CXR
(a) Consolidation (arrows) in the left lower lung zone[25]
(b) Vertical air space consolidation along the left costal margin[27]
(c) Dense consolidation in the right lower zone[25]

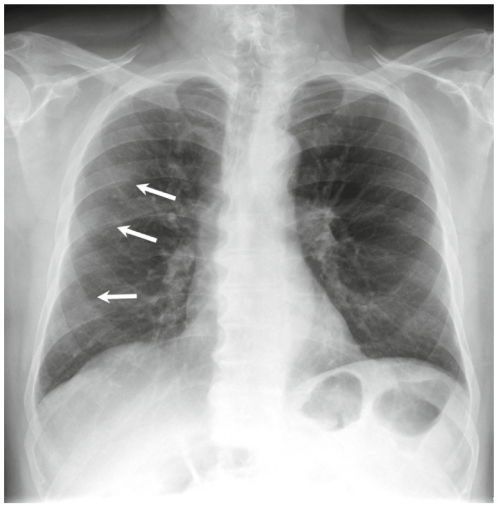

(a) Patchy GGOs with peripheral distribution in the right lung [28]

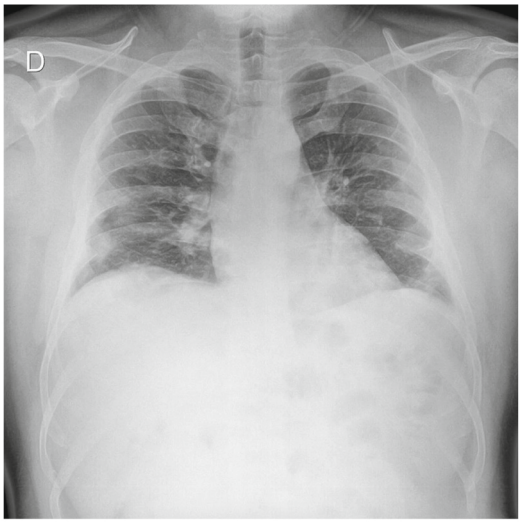

(b) Peripheral GGOs in mid- and lower-third of thorax [29]

(c) Bilateral GGOs more prominent in the right upper lobe and right paramediastinal region [30]

Fig. 3. Cases illustrative of ground-glass opacity (GGO) on CXR
(a) Patchy GGOs with peripheral distribution in the right lung[28]
(b) Peripheral GGOs in mid- and lower-third of thorax[29]
(c) Bilateral GGOs more prominent in the right upper lobe and right paramediastinal region[30]

appearance of consolidation[19].

3.1.3. Bilateral peripheral air opacities

The term "air opacities" is often used in conjunction with "nodules" to denote the filling of air spaces with the products of disease[18]. Compared to community-acquired bacterial pneumoniae, which typically involve one lobe and tend to be unilateral, COVID-19 similar to other viral pneumoniae usually presents with air opacities greater than a single lobe[20]. Recognizing multifocal air opacities on CXR is a pertinent imaging feature of COVID-19 pneumonia. Researchers have noted that the air opacities typically tend to have a bilateral, peripheral and predominantly basal distribution[4] (Fig. 4). Reticular opacities with regions of ground-glass attenuation are usually better visualized on CXR than chest CT[19].

3.1.4. Atypical imaging findings

Pleural effusion is considered to be characteristically rare in COVID-19 and its presence may indicate co-existing bacterial pneumonia[21]. Pleural effusion presents as blunting of the costo-phrenic angle on CXR and often appears as a white area at the lung base. In one study that compared COVID-19 to other viral pneumoniae, pleural effusion was more common in non-COVID-19 viral pneumoniae (Fig. 5)[22]. It may also be a poor prognostic indicator in COVID-19 patients[23].

Pneumothorax is also a rare finding in COVID-19 patients and presents as a thin, sharp white line at the visceral pleural edge (Fig. 5). The authors of one case report of a COVID-19 patient who had a left-sided tension pneumothorax could not be certain whether this pneumothorax was secondary to COVID-19 or the complication was purely coincidental[24]. Atelectasis, cardiomegaly, and pneumomediastinum have also been found in COVID-19 patients; yet, it is to be determined if these are findings are unusual manifestations of COVID-19, a sign of dual pathology, or purely incidental[25].

(a) Bilateral ground-glass alveolar consolidation with peripheral distribution [31]

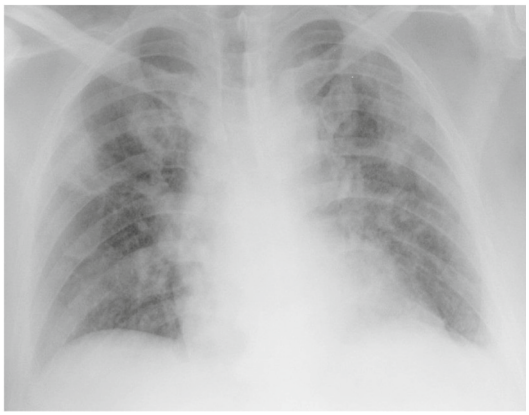

(b) Bilateral ill-defined, patchy alveolar consolidation with peripheral distribution [32]

Fig. 4. Cases illustrative of bilateral peripheral air opacities on CXR
(a) Bilateral ground-glass alveolar consolidation with peripheral distribution[31]
(b) Bilateral ill-defined, patchy alveolar consolidation with peripheral distribution[32]

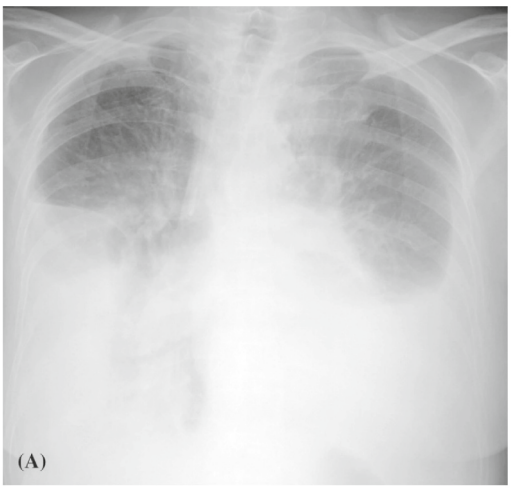

(a) Bilateral pleural effusion and diffuse interstitial thickening [33]

(b) Bilateral pneumothorax and pneumomediastinum with diffuse air space in both lungs [33]

Fig. 5. Cases illustrative of atypical imaging findings on CXR
(a) Bilateral pleural effusion and diffuse interstitial thickening[33]
(b) Bilateral pneumothorax and pneumomediastinum with diffuse air space in both lungs[33]

4. Discussion

Chest radiographs may be found to be "normal" in early or mild disease, however, COVID-19 patients can later develop radiological or clinical signs of viral pneumonia. Seventy-four percent (74%) (95% CI: 51–92%) of patients with COVID-19 had an abnormal CXR at the initial time of diagnosis or sometime during the disease course. Although the number of participants covered by individual COVID-19 CXR studies is low when compared to similarly designed CT studies, a characteristic set of findings are clear. There is no single feature on CXR that is diagnostic of COVID-19 viral pneumonia. Our findings are consistent with meta-analyses of pertinent COVID-19 features on chest CT[18,21], which

suggest that the disease presents as atypical or organizing pneumonia on imaging. The most common abnormalities are consolidation (28%, 95% CI: 8–54%) and ground-glass opacities (29%, 95% CI: 10–53%). The distribution is most frequently bilateral (43%, 95% CI: 27–60%), peripheral (51%, 95% CI: 36–66%), and basal zone (56%, 95% CI: 37–74%) predominant. In contrast to parenchymal abnormalities, pneumothorax (1%, 95% CI: 0–3%) and pleural effusions (6%, 95% CI: 1–16%) are rare.

Our meta-analysis has several strengths. First, the studies, which met the inclusion criteria, occurred in different countries and health centers, providing more generalizable results. Second, the total number of cases was somewhat large for 6 months of early publications, generating an accumulation of evidence to evaluate the diagnosis of COVID-19 by CXR. Third, a variety of different imaging features was gathered, including the distribution patterns in the lungs as well as specific imaging features. However, there are also several limitations. First, the reported imaging findings may not be consistent across studies because of different interpreting radiologists. Second, most of the included studies did not differentiate between COVID-19 patients presenting as clinically mild, moderate, or severe cases. Third, some COVID-19 patients may have had chronic diseases and comorbidities like hypertension and diabetes that could have affected CXR findings.

CXR imaging can play a role in triaging patients due to long PCR turnaround times. Moreover, CXR has several advantages over CT such as cost and practical considerations, which limits CT's utility. The American College of Radiology has noted that CT decontamination, which is required after scanning COVID-19 patients, can disrupt radiology service availability and has suggested that portable CXR be used to reduce the chances of cross-infection[5]. Common CT findings of lower zone predominance, peripheral distribution and bilateral involvement can also be appreciated on CXR[6]. As such, CXR is most likely to be the utilized modality for identification of COVID-19 and follow-up of any associated lung abnormalities[26].

Possible biases in this meta-analysis may be due to the inclusion criteria only using studies published in English, which may exclude data that show different CXR finding trends and patient demographics that could potentially skew the results. In addition, the CXR pathology findings that were analyzed in this study were chosen based on what we considered to be most pertinent based on the various studies that were included, which may leave out possibly common CXR findings. Another possible bias could be the patient demographics, as most studies reported mostly inpatient cases of COVID-19; this possibly narrows the data to more severe cases of COVD-19.

Our results confirm that CXR will continue to be a useful tool in the evaluation and management of patients diagnosed with COVID-19. Although less sensitive than chest CT, CXR can prove useful in its prognostic predictions such as triaging patients and answering questions in regards to whether a patient should stay home, if they will need the ICU in a few days, if they will respond to a specific treatment such as intubation or some drug, whether they should be taken off a ventilator and their overall chances for survival. With an ever-growing number of suspected cases in this pandemic, CXR should be seen as a quick and easy-to-use modality to assess lung abnormalities.

Appendix A. Supplementary data

Supplementary data to this article can be found online at https://doi.org/10.1016/j.clinimag.2021.06.039.

References

1. Coronavirus (COVID-19) events as they happen. https://www.who.int/emergencies/diseases/novel-coronavirus-2019/events-as-they-happen. [Accessed 19 November 2020].
2. He J-L, Luo L, Luo Z-D, et al. Diagnostic performance between CT and initial real-time RT-PCR for clinically suspected 2019 coronavirus disease (COVID-19) patients outside Wuhan, China. Respir Med 2020;168:105980.
3. Rodrigues JCL, Hare SS, Edey A, et al. An update on COVID-19 for the radiologist - a British Society of Thoracic Imaging statement. Clin Radiol 2020;75(5):323–5.
4. Wong HYF, Lam HYS, Fong AH-T, et al. Frequency and distribution of chest radiographic findings in COVID-19 positive patients. Radiology 2019;201160.
5. ACR Recommendations for the use of Chest Radiography and Computed Tomography (CT) for Suspected COVID-19 Infection. https://www.acr.org/Advocacy-and-Economics/ACR-Position-Statements/Recommendations-for-Chest-Radiography-and-CT-for-Suspected-COVID19-Infection. [Accessed 4 June 2020].
6. Sun Z, Zhang N, Li Y, Xu X. A systematic review of chest imaging findings in COVID-19. Quant Imaging Med Surg 2020;10(5):1058–79.
7. Wu Z, McGoogan JM. Characteristics of and important lessons from the coronavirus disease 2019 (COVID-19) outbreak in China: summary of a report of 72 314 cases from the Chinese Center for Disease Control and Prevention. JAMA 2020;323(13):1239–42.
8. Kanne JP, Little BP, Chung JH, Elicker BM, Ketai LH. Essentials for radiologists on COVID-19: an update-radiology scientific expert panel. Radiology 2020:200527.
9. Moher D, Liberati A, Tetzlaff J, Altman DG. Preferred reporting items for systematic reviews and meta-analyses: the PRISMA statement. In: BMJ. British Medical Journal Publishing Group; 2009. p. 339. Accessed August 2, 2020, https://www.bmj.com/content/339/bmj.b2535.
10. Higgins JPT, Thompson SG, Spiegelhalter DJ. A re-evaluation of random-effects meta-analysis. J R Stat Soc Ser A Stat Soc 2009;172(1):137–59.
11. Yoon SH, Lee KH, Kim JY, et al. Chest radiographic and CT findings of the 2019 novel coronavirus disease (COVID-19): analysis of nine patients treated in Korea. Korean J Radiol 2020;21(4):494–500.
12. Chen N, Zhou M, Dong X, et al. Epidemiological and clinical characteristics of 99 cases of 2019 novel coronavirus pneumonia in Wuhan, China: a descriptive study. Lancet Lond Engl. 2020;395(10223):507–13.
13. Guan W, Ni Z, Hu Y, et al. Clinical characteristics of coronavirus disease 2019 in China. N Engl J Med Mass Med Soc 2020;382(18):1708–20.
14. Ng M-Y, Lee EY, Yang J, et al. Imaging profile of the COVID-19infection: radiologic findings and literature review. Radiol Cardiothorac Imaging 2020;2(1). Accessed July 8, 2020, https://www.ncbi.nlm.nih.gov/pmc/articles/PMC7233595/.
15. Ippolito D, Maino C, Pecorelli A, et al. Chest X-ray features of SARS-CoV-2 in the emergency department: a multicenter experience from northern Italian hospitals. Respir Med 2020;170:106036.
16. Toussie D, Voutsinas N, Finkelstein M, et al. Clinical and chest radiography features determine patient outcomes in young and middle age adults with COVID-19. Radiology 2020:201754.
17. Kim ES, Chin BS, Kang CK, et al. Clinical course and outcomes of patients with severe acute respiratory syndrome coronavirus 2 infection: a preliminary report of the first 28 patients from the Korean Cohort Study on COVID-19. J Korean Med Sci 2020;35(13). Accessed July 28, 2020, https://www.ncbi.nlm.nih.gov/pmc/articles/PMC7131901/.
18. Hansell DM, Bankier AA, MacMahon H, McLoud TC, Müller NL, Remy J. Fleischner Society: glossary of terms for thoracic imaging. Radiology 2008;246(3):697–722.
19. Jacobi A, Chung M, Bernheim A, Eber C. Portable chest X-ray in coronavirus disease-19 (COVID-19): a pictorial review. Clin Imaging 2020;64:35–42.
20. Vilar J, Domingo ML, Soto C, Cogollos J. Radiology of bacterial pneumonia. Eur J Radiol 2004;51(2):102–13.
21. Blachford A. Chest X-Ray findings among urgent care patients with COVID-19 are not affected by patient age or gender: a retrospective cohort study of 636 ambulatory patients. J Urgent Care Med 2020. Accessed July 5, 2020, https://www.jucm.com/chest-x-ray-findings-among-urgent-care-patients-with-covid-19-are-not-affected-by-patient-age-or-gender-a-retrospective-cohort-study-of-636-ambulatory-patients/.
22. Cascella M, Rajnik M, Cuomo A, Dulebohn SC, Di Napoli R. Features, Evaluation and Treatment Coronavirus (COVID-19). StatPearls. Treasure Island (FL): StatPearls Publishing; 2020. Accessed July 29, 2020, http://www.ncbi.nlm.nih.gov/books/NBK554776/.

[23] Litmanovich DE, Chung M, Kirkbride R, Kicska G, Kanne PJ. Review of chest radiograph findings of COVID-19 pneumonia and suggested reporting language. Publish Ahead of Print J Thorac Imaging 2020;35(6):354–60. Accessed July 4, 2020, https://journals.lww.com/thoracicimaging/Abstract/9000/Review_of_Chest_Radiograph_Findings_of_COVID_19.99401.aspx.

24. Flower L, Lopez JR, Henry AM, Carter J-PL. Tension pneumothorax in a patient with COVID-19. BMJ Case Rep CP BMJ Specialist J 2020;13(5):e235861.
25. Cleverley J, Piper J, Jones MM. The role of chest radiography in confirming covid-19 pneumonia. In: BMJ. 370. British Medical Journal Publishing Group; 2020. Accessed July 29, 2020, https://www.bmj.com/content/370/bmj.m2426.
26. Kooraki S, Hosseiny M, Myers L, Gholamrezanezhad A. Coronavirus (COVID-19) outbreak: what the Department of Radiology should know. J Am Coll Radiol JACR. 2020;17(4):447–51.
27. Nicoletti D. COVID-19 pneumonia | Radiology Case | Radiopaedia.org. Radiopaedia. https://radiopaedia.org/cases/covid-19-pneumonia-7. [Accessed 11 July 2020].
28. Khan MI. Post-intubation pneumomediastinum and pneumothorax - background COVID-19 pneumonia | Radiology Case | Radiopaedia.org. Radiopaedia. https://radiopaedia.org/cases/post-intubation-pneumomediastinum-and-pneumothorax-background-covid-19-pneumonia?lang=us. [Accessed 13 July 2020].
29. Patel R. COVID 19 Pneumonia | Radiology Case | Radiopaedia.org. Radiopaedia. https://radiopaedia.org/cases/covid-19-pneumonia-67?lang=us. [Accessed 13 July 2020].
30. Creus AA. COVID-19 pneumonia | Radiology Case | Radiopaedia.org. Radiopaedia. https://radiopaedia.org/cases/covid-19-pneumonia-22?lang=us. [Accessed 12 July 2020].

31. Lorente E. COVID-19 pneumonia | Radiology Case | Radiopaedia.org. Radiopaedia. https://radiopaedia.org/cases/covid-19-pneumonia-20?lang=us. [Accessed 9 July 2020].
32. Lorente E. COVID-19 pneumonia - evolution over a week | Radiology Case | Radiopaedia.org. Radiopaedia. https://radiopaedia.org/cases/covid-19-pneumonia-evolution-over-a-week-1. [Accessed 11 July 2020].
33. Bell DJ. COVID-19 | Radiology Reference Article | Radiopaedia.org. Radiopaedia. https://radiopaedia.org/articles/covid-19-4. [Accessed 19 November 2020].